

3-N-butylphthalide inhibits neuronal apoptosis in rats with cerebral infarction via targeting P38/MAPK

W. LIAO¹, Y. ZHONG², W. CHENG¹, L.-F. DONG³

¹Department of Neurosurgery, The First Affiliated Hospital of Gannan Medical University, Ganzhou, China

²Scientific Research Management Division, The First Affiliated Hospital of Gannan Medical University, Ganzhou, China

³Ganzhou People's Hospital, Ganzhou, China

Abstract. – **OBJECTIVE:** To study the effect of 3-n-butylphthalide (NBP) on neuronal apoptosis in rats with cerebral infarction (CI) through the p38/mitogen-activated protein kinase (MAPK) pathway. **MATERIALS AND METHODS:** A total of 30 rats were divided into control group (healthy rats, n=10), model group (CI rat model, n=10), and NBP group (CI rat model + intraperitoneal injection of NBP, n=10). Then, the neurological function, degree of cerebral ischemia, apoptosis of brain tissues, the protein and messenger ribonucleic acid (mRNA) expressions of p-p38 and MAPK in brain tissues were detected using the neurological score, 2,3,5-triphenyltetrazolium chloride (TTC) staining, Reverse Transcription-Polymerase Chain Reaction (RT-PCR), terminal deoxynucleotidyl transferase-mediated dUTP nick end labeling (TUNEL) assay, and Western blotting, respectively.

RESULTS: In NBP group, the neurological score was significantly lower than in model group, and the difference was statistically significant ($p<0.05$). The results of TTC staining revealed that the area of the white region in brain slices was significantly larger in model group than in control group, indicating the successful establishment of middle cerebral artery occlusion (MCAO) model. Compared with model group, NBP group had a smaller area and lighter color of the white region in brain slices, suggesting that NBP markedly reduces the MCAO-induced CI. The apoptosis rate in NBP group was higher than in control group ($p<0.05$), but lower than in model group ($p<0.05$), while it was higher in model group than in control group ($p<0.05$). The protein expressions of p38 and MAPK in NBP group were higher than in control group ($p<0.05$), but lower than in model group ($p<0.05$), while they were higher in model group than in control group ($p<0.05$). Moreover, the mRNA expressions of p38 and MAPK were lower in control group than in model group ($p<0.05$), while they were higher in model group than in

NBP group ($p<0.05$), but there was no significant difference in the mRNA expression of p38 between NBP group and control group ($p>0.05$).

CONCLUSIONS: NBP alleviates neuronal apoptosis in CI by down-regulating the p38 signal and inhibiting the expression of MAPK, thereby treating CI.

Key Words:

3-n-butylphthalide, P38/MAPK, Cerebral infarction, Neuronal apoptosis.

Introduction

Cerebral infarction (CI) is one of the leading causes of residents' death in China¹. Brain tissues are very sensitive to thrombus, which can cause irreversible neurological damage². CI is characterized by a short time of thrombolysis, high mortality, and disability rates³. CI results in permanent disability in 80% of patients and about 35% of them cannot take care of themselves⁴, which is also the key and difficulty in clinical research on CI. There are many pathogenesises of CI and it may be caused by local thrombus in brain tissues, thus leading to the necrosis of brain tissues⁵. 3-n-butylphthalide (NBP) is a therapeutic drug for CI developed by China⁶. It has been clinically confirmed that NBP has high safety and can well improve the cognitive function and behavioral outcomes of CI patients⁷. Many studies⁸ have proved the neuroprotective role of NBP and some mechanisms have also been revealed. NBP can alter the area of CI, remarkably improve the neurological function of CI rats, and inhibit the neuronal apoptosis, demonstrating that NBP possesses

a cerebral protective effect⁹. The p38 signaling pathway is a member of the mitogen-activated protein kinase (MAPK) pathway, and it was found in the perfusion model experiment that inhibiting the p38 pathway can protect neurons¹⁰. Moreover, NBP can inhibit the increase in the level of phosphorylated p38 (p-p38) MAPK protein in brain tissues and alleviate cerebral injury in rats¹¹. It has been confirmed that the expression of the most characteristic p38 pathway is activated in neurons during CI perfusion¹². The present work aims to explore the correlation between the p38/MAPK pathway and the pathogenesis of CI, as well as the effect of NBP on CI, to provide a new basis for clinical treatment.

Materials and Methods

Laboratory Animals

A total of 30 healthy adult female Sprague-Dawley rats weighing 180-220 g and aged 6-8 weeks old were provided by the Shandong Laboratory Animal Center, and they were fed in separate cages in the specific pathogen-free animal room under the room temperature of (22 ± 2)°C, humidity of 50-60%, and 12/12 h light/dark cycle. Also, they had free access to food and water. This investigation was approved by the Animal Ethics Committee of Gannan Medical University at the Ganzhou Animal Center.

Main Reagents and Drugs

NBP was purchased from Jiangsu Hengrui Medicine Co., Ltd. (Nanjing, China), rabbit anti-p38 antibody from Merck Millipore (Billerica, MA, USA), rat anti-MAPK antibody from EarthOx (Hyclone, South Logan, UT, USA), bovine serum albumin (BSA) from Beijing Dingguo Pharmaceutical Co., Ltd. (Beijing, China), 70% medicinal alcohol from Xinxiang Zhongcheng Company (Xinxiang, China), drying oven from Beijing Chuankang Company (Beijing, China), a balance from Shandong Anping Pharmaceutical Co., Ltd. (Heze, China), a sterilizer, and an injector from Nanjing Anyang Company (Nanjing, China).

Experimental Grouping and Drug Administration

Thirty rats were divided into control group (healthy rats, n=10), model group (CI rat model, n=10), and NBP group (CI rat model + intraperitoneal injection of NBP, n=10) using a random

number table. In control group, the middle cerebral artery occlusion (MCAO) was not performed, but 1.2 mL of normal saline was intraperitoneally injected. In model group, the MCAO model was established and 1.2 mL of normal saline was also intraperitoneally injected. In NBP group, NBP (15 mg/kg) was injected intraperitoneally at 3 h before MCAO modeling.

MCAO Modeling Method

After weighing and intraperitoneal injection of 5% chloral hydrate (0.07 mL/10 g), the rats were fixed in the supine position, the neck was disinfected with iodine, and a median neck incision was made. The submandibular glands were bluntly dissected and pulled to one side with a small hook. The left common carotid artery (CCA) was bluntly dissected and ligated in a slipknot. The external carotid artery (ECA) was dissociated and its distal end was ligated, while a slipknot was made in its proximal end. Next, the slipknot in CCA was pulled tightly and an incision was made in main ECA using micro-scissors, the suture was inserted into the proximal end of ECA along the incision to the CCA, and the ligature was pulled tightly. The ECA was cut off at the distal end, the suture was gently pulled back and twisted at a specific angle, making an obtuse angle between ECA and internal carotid artery (ICA). Then, the ligature at ICA was loosened and the suture was slowly sent to ICA through the furcation of CCA. The incoming end of suture was tightened to prevent shedding. The excess external ligature was cut off, the glands were put back in place, and the wound was sutured and moisturized with normal saline using cotton swabs. At 2 h after cerebral ischemia, the suture was slowly pulled out, the ligature at ECA and CCA was loosened and removed for reperfusion after ischemia. The skin was sutured and the rats were placed in separate cages for resuscitation (note the post-operative warming). After 24 h, the behavioral functions of rats were evaluated.

Behavioral Function Score

The symptoms of neurological deficits were observed and recorded at 24 h after perfusion using the single-blind method. Neurological score: 0 point: no neurological deficits, 1 point: mild neurological deficits, 2 points: moderate neurological deficits, 3 points: severe neurological deficits, and 4 points: loss of neurological function (Table I).

Table I. Neurological score.

Site	Condition	Score
Left forelimb	Normal limb function	0 point
Left forelimb	The left forelimb bends and cannot be fully stretched in tail suspension	1 point
Leg	Rotate while walking, and able to keep balance when standing still	2 points
Leg	Tilt to the left while walking, unstable when standing	3 points
Leg	Unable to walk spontaneously, and lose consciousness	4 points

Reverse Transcription-Quantitative Polymerase Chain Reaction (RT-qPCR)

The expression of p38 in brain tissues in the three groups was detected *via* RT and qPCR. The tissue samples in the cryopreserved tube were taken, drained, and placed in the 5 mL tube. After complete homogenization using a tissue homogenizer, the liquid was transferred into the clean imported 1.5 mL Eppendorf (EP) tube and placed at room temperature for 5-10 min for complete lysis, followed by centrifugation at 1,200 rpm for 5 min. Subsequently, the precipitate was discarded. Chloroform and TRIzol (Invitrogen, Carlsbad, CA, USA) were added (200 μ L of chloroform/mL TRIzol) to prepare the chloroform/TRIzol reagent. Also, they were shaken and mixed evenly, placed at room temperature for 15 min, and centrifuged at 12,000 rpm and 4°C for 15 min. Then, the supernatant was aspirated into another centrifuge tube, added with isopropanol (0.7-1-fold volume of the supernatant), placed at room temperature for 10-30 min, and centrifuged at 12,000 rpm for 10 min. The supernatant was discarded and ribonucleic acids (RNAs) were precipitated to the bottom of the tube. Then, 75% ethanol (1 mL of 75% ethanol/mL TRIzol) was added into the centrifuge tube, gently shaken to suspend the precipitates, and centrifuged at 12,000 rpm and 4°C for 5 min. The supernatant was discarded as much as possible, the precipitates were blown dry on a super clean bench for 10-20 min, and dissolved using 10-50 μ L of diethyl pyrocarbonate-treated ddH₂O. The concentration was detected using OneDrop micro-spectrophotometer. Reverse transcription (RT) reaction was performed using 4.5 μ L of RNase-free ddH₂O, 2 μ L of 5 \times RT reaction buffer, 0.5 μ L of random primers, 0.5 μ L of Oligo dT, 0.5 μ L of reverse transcriptase and 2 μ L of RNAs. The complementary deoxyribonucleic acids (cDNAs) samples were divided into three portions (diluted at 1:20). 3 μ L of cDNA was taken for PCR amplification. The amplification

level of the target gene was verified *via* 5% agarose gel electrophoresis. Then, the LabWorks 4.0 image acquisition and analysis software were used for quantification and data processing. To obtain reliable data, the experiment was performed for three times in each group. In the present research, the changes in the relative expression levels of target genes were analyzed using the 2^{- $\Delta\Delta$ Ct} method. The primer sequences used are shown in Table II.

2,3,5-Triphenyltetrazolium Chloride (TTC) Staining

The rats were sacrificed *via* dislocation at one time, the brain tissues were separated, and the excess tissues were carefully removed. The brain tissues were quickly frozen in a refrigerator at -80°C for about 20 min, followed by the preparation of sections. The intact brain was sliced into 5 pieces, placed in TTC dye at a concentration of 2%, and covered with the silver paper for incubation in a dark place, followed by a water bath at 37°C for 15 min. The sections were turned over from time to time to allow them to uniformly contact the staining solution.

Detection of Neuronal Apoptosis in Each Group Via Terminal Deoxynucleotidyl Transferase-Mediated dUTP Nick End Labeling (TUNEL) Assay

The brain tissues were embedded in paraffin and serially sliced into three 5 μ m-thick paraffin sections. The paraffin sections were examined

Table II. Gene primer sequences.

Gene	Primer sequence
Bcl-2	5'-CCG GAG CTG AAT GAC GCT CTC AGG-3' 5'-TAC TGT AAT GTT TTG ATT TCA TTG-3'
Bax	5'-CTT AGG GCT GAG CTG GTG GAC GCT-3' 5'-ATT TCA TTG AAT GTT TAC TTG TGT-3'
β -actin	5'-CTC CTC TTG CTC GAT AGT CTC TCG-3' 5'-TCG ATG TCG AAG ACC TTC TTC AAC-3'

for apoptosis of brain tissues in each group via TUNEL assay according to the instructions. Five uncrossed non-repeated fields were randomly selected on each pathological section, and observed under a light microscope. The light brown cells were apoptotic cells. Also, the apoptosis rate was calculated: apoptotic cell count/total cell count \times 100%.

Detection of Changes in p38 and p-p38 Protein Expressions Via Western Blotting

An appropriate amount of radio immunoprecipitation assay (RIPA) lysis buffer was prepared and the protease inhibitor phenylmethane-sulfonyl fluoride (PMSF; RIPA: PMSF = 100:1) was added and mixed evenly. After the brain tissues were separated and cut into pieces, the lysis buffer was added (10:1), and the lysate was collected and transferred into an EP tube using a tissue homogenizer, followed by centrifugation at 14,000 rpm and 4°C for 30 min using the refrigerated high-speed centrifuge. Then, the protein supernatant was collected and subjected to a heating bath at 95°C for 10 min for protein denaturation. The protein samples prepared were placed in a refrigerator at -80°C for later use, while the protein was quantified using the bicinchoninic acid (BCA) kit (Pierce, Rockford, IL, USA). After that, the dodecyl sulfate, sodium salt-polyacrylamide gel electrophoresis (SDS-PAGE) gel was prepared and the protein samples were loaded into the gel loading well for electrophoresis under the constant voltage of 80 V for 2.5 h. Then, the protein was transferred onto polyvinylidene difluoride (PVDF) membranes using a semi-dry transfer method (Millipore, Billerica, MA, USA). The PVDF membrane was immersed in Tris-Buffered Saline and Tween (TBST) containing 5% skim milk powder and shaken slowly for 1 h on a shaking table to be sealed. Next, the protein was incubated with the primary antibody diluted with 5% skim milk powder, rinsed with TBST for 3 times (10 min/time), incubated again with the secondary antibody at room temperature for 2 h. Also, it was rinsed again with TBST twice and with TBS once (10 min/time). Finally, the protein was detected using the enhanced chemiluminescence (ECL) reagent, followed by exposure in a dark room. The relative expression of the protein was analyzed using Image-Pro Plus v6 (Media Cybernetics, Silver Spring, MD, USA).

Statistical Analysis

Three parallel groups or three replicates were set up in all experiments. The results were expressed as mean \pm standard deviation ($\chi \pm$ SD), and *t*-test was used for the intergroup comparison of statistical difference. $p < 0.05$ suggested that the difference had statistical significance and $p < 0.01$ suggested that the difference had a great statistical significance.

Results

Neurological Score

The neurological score was 0, (3.1 ± 0.46) and (1.15 ± 0.28) points, respectively, in control group, model group, and NBP group. It can be seen that the neurological score in NBP group was significantly lower than in model group, and the difference was statistically significant ($p < 0.05$) (Table III).

TTC Staining

The results of TTC staining revealed that the area of the white region in brain slices was evidently larger in model group than in control group, indicating the successful establishment of the MCAO model. Compared with model group, NBP group had a smaller area and lighter color of the white region in brain slices, suggesting that NBP evidently reduces the MCAO-induced CI (Figure 1)

Effect of NBP on MCAO-Induced Neuronal Apoptosis in Brain Tissues Detected Via TUNEL Assay

The apoptosis rate was markedly higher in model group than that in control group, showing a statistically significant difference ($p < 0.05$), while it was significantly lower in NBP group than that in model group, also showing a statistically significant difference ($p < 0.05$), suggesting that NBP can markedly reduce MCAO-induced neuronal apoptosis of rats (Figure 2).

Table III. Comparison of neurological score among groups.

Group	Neurological score
Control group	0
Model group	$3.1 \pm 0.46^*$
NBP group	$1.15 \pm 0.28^{*#}$

Note: * $p < 0.05$ vs. control group, # $p < 0.05$ vs. model group.



Figure 1. TTC staining results.

Differences in Messenger RNA (mRNA) Expressions of Bcl-2 and Bax in Brain Tissues Detected Via RT-qPCR

Bax/Bcl-2 mRNA expression was remarkably increased in model group compared with that in control group, displaying a statistically significant difference ($p < 0.05$), while it was remarkably decreased in NBP group compared with that in

model group, also displaying a statistically significant difference ($p < 0.05$) (Figure 3).

P-p38 and p38 Protein Expressions in Brain Tissues Detected Via Western Blotting

The p-p38/p38 expression was remarkably increased in model group compared with that in

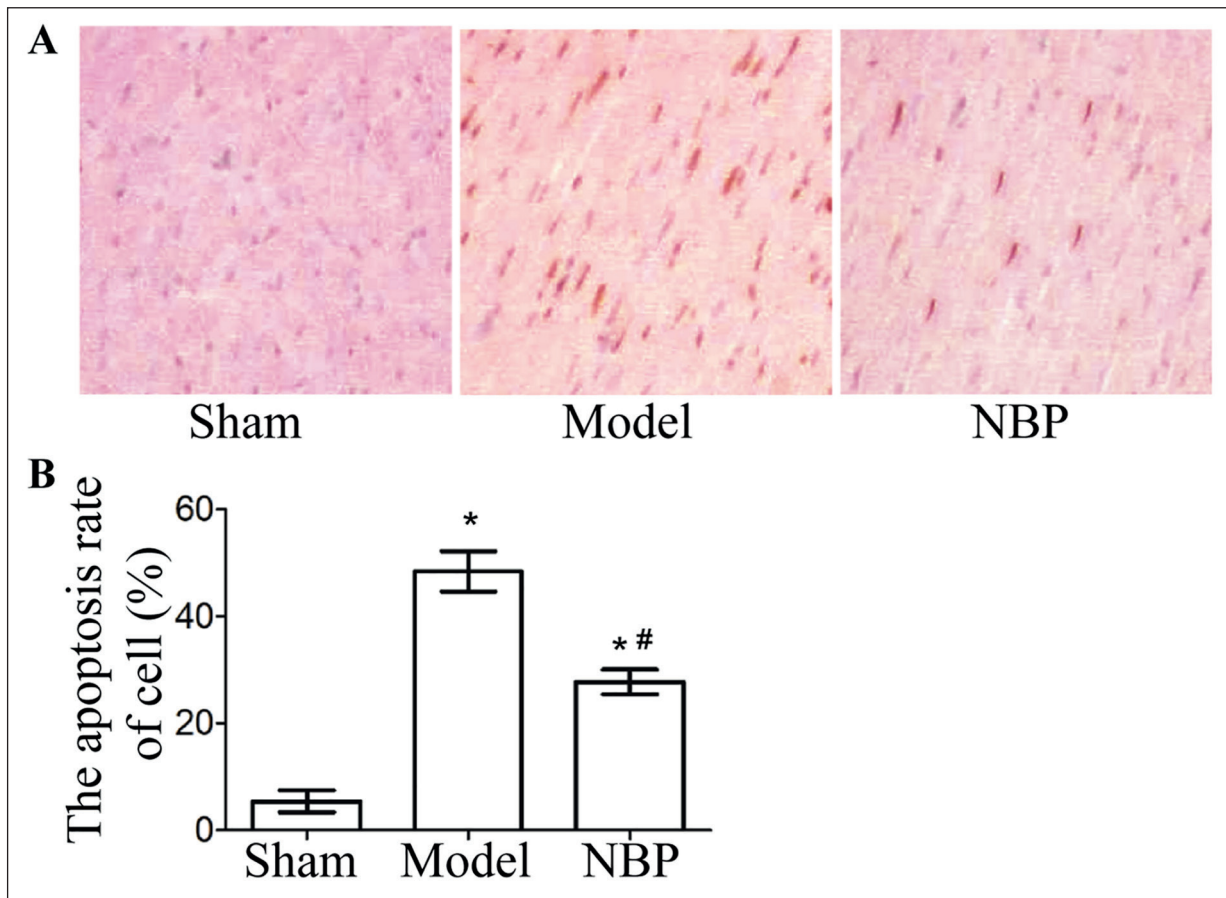


Figure 2. Effect of NBP on MCAO-induced neuronal apoptosis in brain tissues detected *via* TUNEL assay. **A**, Number of apoptotic cells (magnification: 200 \times), **B**, comparison of apoptosis rate among groups. * $p < 0.05$ vs. control group, # $p < 0.05$ vs. model group.

control group, displaying a statistically significant difference ($p < 0.05$), while it was remarkably decreased in NBP group compared with that in model group, with a statistically significant difference ($p < 0.05$) (Figures 3 and 4).

Discussion

According to reports¹³, CI has a high mortality rate among a large number of diseases. The disability and recurrence rates of CI have increased year by year, making CI a health problem to be urgently solved in China. Effective treatment means can promote the recovery of neurological function¹⁴. The endogenous repair mechanism is an important issue we face. Indeed, it is the purpose of the research. According to the experimental results in the present study, the neurological score in NBP group was significantly lower than in model group, and the difference

was statistically significant ($p < 0.05$). The nerve cell membrane was intact in control group, the number of nuclei was smaller in model group

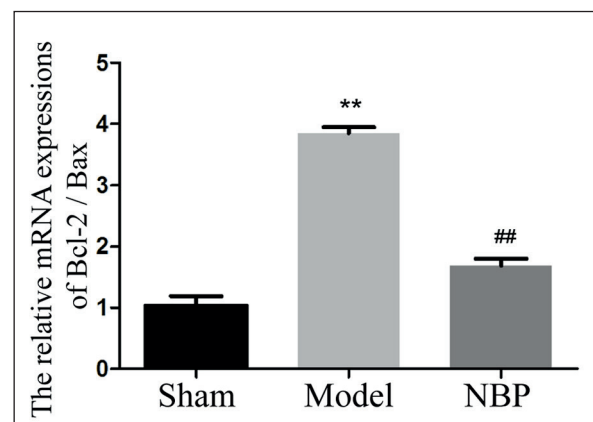


Figure 3. Differences in mRNA expressions of Bcl-2 and Bax in brain tissues detected *via* RT-qPCR. ** $p < 0.01$ model group vs. control group, ## $p < 0.01$ NBP group vs. model group.

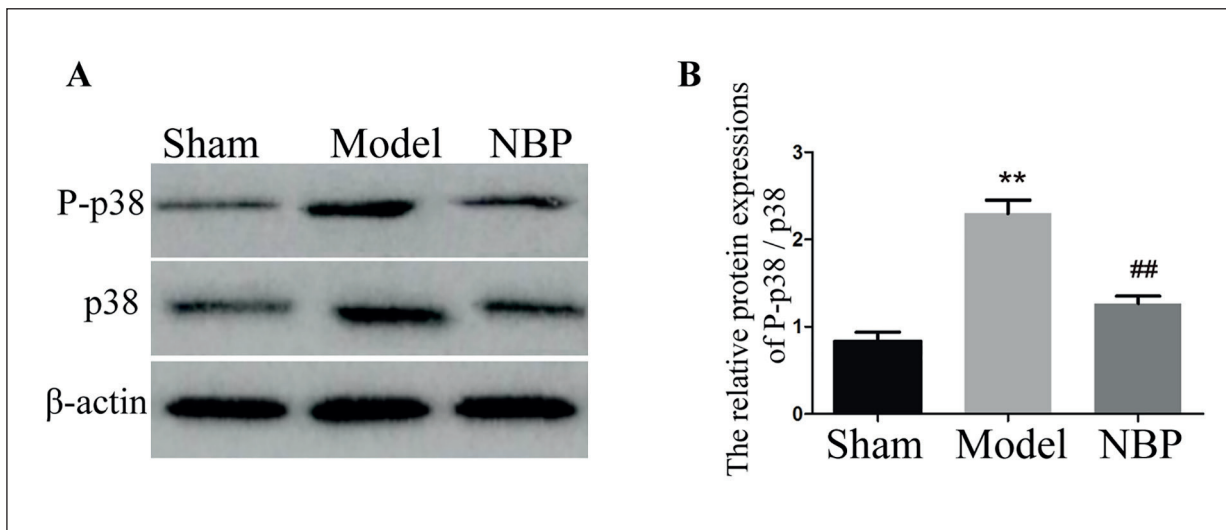


Figure 4. P-p38 and p38 protein expressions in brain tissues detected via Western blotting. ** $p < 0.01$ model group vs. control group, ## $p < 0.01$ NBP group vs. model group.

than in control group, and the neuronal edema in NBP group was evidently relieved compared with that in model group. The apoptosis rate was lower in NBP group than in model group ($p < 0.05$), higher in model group than in control group ($p < 0.05$), and also higher in NBP group than in control group ($p < 0.05$). Moreover, the NBP treatment could significantly improve the neurological function of CI rats in the experiment, suggesting that the NBP treatment has a cerebral protective effect¹⁵. NBP intervention can markedly increase the number of dendritic branches in the cortex at the center of and around the infarction. The increase in NBP can raise the density, length, and width of dendritic spines in the cortex around the infarction¹⁶. It has been observed¹⁷, through staining, that NBP can improve the growth of dendrites and axons in the cortex around the infarction towards the center of infarction, demonstrating that NBP is able to facilitate neuroplasticity. The results of Western blotting manifested that the protein expressions of p38 and MAPK in brain tissues in NBP group were higher than in control group ($p < 0.05$), but lower than in model group ($p < 0.05$), while they were higher in model group than in control group ($p < 0.05$), confirming the positive correlation between p38 and MAPK. It was found in RT-PCR that the mRNA expressions of p38 and MAPK were lower in control group than in model group ($p < 0.05$), while they were higher in model group than in NBP group ($p < 0.05$); however, there was no significant difference in the mRNA expression

of p38 between NBP group and control group ($p > 0.05$). The p38 signaling pathway is a member of the MAPK pathway. In the study on CI perfusion model, inhibiting the p38 pathway can exert a protective effect on neurons¹⁸. Currently, it has been demonstrated¹⁹ that the expression of the most characteristic p38/MAPK pathway is activated in astrocytes and neurons during CI perfusion. Kulanuwat et al²⁰ found that a variety of apoptosis-related genes can be activated by activating the kinase expression, while apoptosis can be alleviated by retardants to some extent, indicating that p38 is related to apoptosis. Studies²¹ have found that reactive oxygen species produced in CI can activate p38 to be involved in target cell damage during CI. Yamamoto et al²² analysed the isoflurane-induced cerebral injury in rats and found that the p38 signaling pathway is involved in the process of neuronal apoptosis. In the rat model of MCAO, perfusion can increase the expression of p38 in the infarction region, while the tolerance of neurons in this region to thrombus is weakened, and inhibiting the p38 expression can enhance the protection on neurons²³. Besides, the expression of MAPK begins to increase after CI perfusion in rats, suggesting that MAPK promotes apoptosis after CI. Also, MAPK is involved in neuronal apoptosis after CI²⁴. AlHaj et al²⁵ showed that the expression of MAPK in brain tissues in the thrombus region in rats with focal CI perfusion injury is increased, indicating that CI perfusion injury can result in high expression of MAPK in brain tissues in the thrombus

region. After NBP treatment, the expression of MAPK in brain tissues in the thrombus region in rats with focal CI perfusion injury declines, demonstrating that NBP treatment can suppress the expression of MAPK in brain tissues in the thrombus region²⁶.

Conclusions

We showed that NBP alleviated neuronal apoptosis in CI by down-regulating the p38 signal and inhibiting the expression of MAPK, thereby treating CI.

Conflict of Interest

The Authors declare that they have no conflict of interests.

References

- 1) GUO X, XIANG Y, YANG H, YU L, PENG X, GUO R. Association of the LOX-1 rs1050283 polymorphism with risk for atherosclerotic cerebral infarction and its effect on sLOX-1 and LOX-1 expression in a Chinese population. *J Atheroscler Thromb* 2017; 24: 572-582.
- 2) ZHANG Y, QIU B, WANG J, YAO Y, WANG C, LIU J. Effects of BDNF-Transfected BMSCs on neural functional recovery and synaptophysin expression in rats with cerebral infarction. *Mol Neurobiol* 2017; 54: 3813-3824.
- 3) BOND MJ, BLEILER M, HARRISON LE, SCOCCHERA EW, NAKANISHI M, G-DAYANAN N, KESHIPEDDY S, ROSENBERG DW, WRIGHT DL, GIARDINA C. Spindle assembly disruption and cancer cell apoptosis with a CLTC-binding compound. *Mol Cancer Res* 2018; 16: 1361-1372.
- 4) WANG J, XIE Y, ZHAO S, ZHANG J, CHAI Y, LI Y, LIAO X. Dengzhanxin injection for cerebral infarction: a systematic review and meta-analysis of randomized controlled trials. *Medicine (Baltimore)* 2017; 96: e7674.
- 5) LU G, WONG MS, XIONG MZQ, LEUNG CK, SU XW, ZHOU JY, POON WS, ZHENG VZY, CHAN WY, WONG GKC. Circulating microRNAs in delayed cerebral infarction after aneurysmal subarachnoid hemorrhage. *J Am Heart Assoc* 2017; 6: pii: e005363.
- 6) HU J, WEN Q, WU Y, LI B, GAO P. The effect of butylphthalide on the brain edema, blood-brain barrier of rats after focal cerebral infarction and the expression of Rho A. *Cell Biochem Biophys* 2014; 69: 363-368.
- 7) NIU H, ZHANG Z, WANG H, WANG H, ZHANG J, LI C, ZHAO L. The impact of butylphthalide on the hypothalamus-pituitary-adrenal axis of patients suffering from cerebral infarction in the basal ganglia. *Electron Physician* 2016; 8: 1759-1763.
- 8) ZHANG C, ZHAO S, ZANG Y, GU F, MAO S, FENG S, HU L, ZHANG C. The efficacy and safety of DL-3n-butylphthalide on progressive cerebral infarction: a randomized controlled STROBE study. *Medicine (Baltimore)* 2017; 96: e7257.
- 9) TANG SC, LUO CJ, ZHANG KH, LI K, FAN XH, NING LP, XUE P. Effects of dl-3-n-butylphthalide on serum VEGF and bFGF levels in acute cerebral infarction. *Eur Rev Med Pharmacol Sci* 2017; 21: 4431-4436.
- 10) FANNING JP, WESLEY AJ, WALTERS DL, WONG AA, BARNETT AG, STRUGNELL WE, PLATTS DG, FRASER JF. Topographical distribution of perioperative cerebral infarction associated with transcatheter aortic valve implantation. *Am Heart J* 2018; 197: 113-123.
- 11) LEE XR, XIANG GL. Effects of edaravone, the free radical scavenger, on outcomes in acute cerebral infarction patients treated with ultra-early thrombolysis of recombinant tissue plasminogen activator. *Clin Neurol Neurosurg* 2018; 167: 157-161.
- 12) FANNING JP, SEE HL, PASSMORE MR, BARNETT AG, ROLFE BE, MILLAR JE, WESLEY AJ, SUEN J, FRASER JF. Differential immunological profiles herald magnetic resonance imaging-defined perioperative cerebral infarction. *Ther Adv Neurol Disord* 2018; 11: 1756286418759493.
- 13) KIM SW, KIM CM, KIM DM, YUN NR. Manifestation of anaplasmosis as cerebral infarction: a case report. *BMC Infect Dis* 2018; 18: 409.
- 14) YASUKOCHI Y, SAKUMA J, TAKEUCHI I, KATO K, OGURI M, FUJIMAKI T, HORIBE H, YAMADA Y. Six novel susceptibility loci for coronary artery disease and cerebral infarction identified by longitudinal exome-wide association studies in a Japanese population. *Biomed Rep* 2018; 9: 123-134.
- 15) SONG FX, WANG L, LIU H, WANG YL, ZOU Y. Brain cell apoptosis inhibition by butylphthalide in Alzheimer's disease model in rats. *Exp Ther Med* 2017; 13: 2771-2774.
- 16) FENG L, SHARMA A, NIU F, HUANG Y, LAFUENTE JV, MURESANU DF, OZKIZILCIK A, TIAN ZR, SHARMA HS. TiO2-nanowired delivery of DL-3-n-butylphthalide (DL-NBP) attenuates blood-brain barrier disruption, brain edema formation, and neuronal damages following concussive head injury. *Mol Neurobiol* 2018; 55: 350-358.
- 17) ZHANG X, LI Y, LI X, RONG X, TANG Y, PENG Y. NEUROPROTECTIVE EFFECT OF DL-3-N-BUTYLPHTHALIDE ON PATIENTS WITH RADIATION-INDUCED BRAIN INJURY: A CLINICAL RETROSPECTIVE COHORT STUDY. *Int J Neurosci* 2017; 127: 1059-1064.
- 18) MATSUMOTO K, SATO S, OKUMURA M, NIWA H, HIDA Y, KAGA K, DATE H, NAKAJIMA J, USUDA J, SUZUKI M, SOUMA T, TSUCHIDA M, MIYATA Y, NAGAYASU T. Frequency of cerebral infarction after pulmonary resection: a multicenter, retrospective study in Japan. *Surg Today* 2018; 48: 571-572.

- 19) KAKUDO T, KISHIMOTO N, MATSUYAMA T, MOMOTA Y. Functional recovery by application of human de-differentiated fat cells on cerebral infarction mice model. *Cytotechnology* 2018; 70: 949-959.
- 20) KULANUWAT S, JUNGTRAKOON P, TANGJITTIPOKIN W, YENCHITSOMANUS PT, PLENGVIDHYA N. Fanconi anemia complementation group C protection against oxidative stress-induced β -cell apoptosis. *Mol Med Rep* 2018; 18: 2485-2491.
- 21) MURAOKA S, ARAKI Y, KONDO G, KURIMOTO M, SHIBA Y, UDA K, OTA S, OKAMOTO S, WAKABAYASHI T. Postoperative cerebral infarction risk factors and post-operative management of pediatric patients with Moyamoya disease. *World Neurosurg* 2018; 113: e190-e199.
- 22) YAMAMOTO T, IWAMOTO T, KIMURA S, NAKAO S. Persistent isoflurane-induced hypotension causes hippocampal neuronal damage in a rat model of chronic cerebral hypoperfusion. *J Anesth* 2018; 32: 182-188.
- 23) REINSFELT B, WESTERLIND A, HOULTZ E, EDERBERG S, ELAM M, RICKSTEN SE. The effects of isoflurane-induced electroencephalographic burst suppression on cerebral blood flow velocity and cerebral oxygen extraction during cardiopulmonary bypass. *Anesth Analg* 2003; 97: 1246-1250.
- 24) MAHALE R, MEHTA A, SHETTY N, SRINIVASA R. Does cerebral infarction ameliorate essential tremor? A mini-review. *Neurol India* 2018; 66 (Supplement): S152-S154.
- 25) ALHAJ HOUSSEN A, ALGREESHAH F. Aspergillus sinusitis complicated with meningitis and multiple cerebral infarctions in immunocompetent patient. *Neurosciences (Riyadh)* 2018; 23: 148-151.
- 26) CHENG CY, TANG NY, KAO ST, HSIEH CL. Ferulic acid administered at various time points protects against cerebral infarction by activating p38 MAPK/p90RSK/CREB/Bcl-2 anti-apoptotic signaling in the subacute phase of cerebral ischemia-reperfusion injury in rats. *PLoS One* 2016; 11: e0155748.